OPEN

Citation: Cell Death and Disease (2013) 4, e940; doi:10.1038/cddis.2013.463

www.nature.com/cddis

# Caspase-2 promotes cytoskeleton protein degradation during apoptotic cell death

H Vakifahmetoglu-Norberg*[,1,6,7], E Norberg[1,6,7,8], AB Perdomo[2], M Olsson[1], F Ciccosanti[2], S Orrenius[1], GM Fimia[2,3], M Piacentini[2,4] and B Zhivotovsky*[,1,5]

**The caspase family of proteases cleaves large number of proteins resulting in major morphological and biochemical changes during apoptosis. Yet, only a few of these proteins have been reported to selectively cleaved by caspase-2. Numerous observations link caspase-2 to the disruption of the cytoskeleton, although it remains elusive whether any of the cytoskeleton proteins serve as *bona fide* substrates for caspase-2. Here, we undertook an unbiased proteomic approach to address this question. By differential proteome analysis using two-dimensional gel electrophoresis, we identified four cytoskeleton proteins that were degraded upon treatment with active recombinant caspase-2 *in vitro.* These proteins were degraded in a caspase-2-dependent manner during apoptosis induced by DNA damage, cytoskeleton disruption or endoplasmic reticulum stress. Hence, degradation of these cytoskeleton proteins was blunted by siRNA targeting of caspase-2 and when caspase-2 activity was pharmacologically inhibited. However, none of these proteins was cleaved directly by caspase-2. Instead, we provide evidence that in cells exposed to apoptotic stimuli, caspase-2 probed these proteins for proteasomal degradation. Taken together, our results depict a new role for caspase-2 in the regulation of the level of cytoskeleton proteins during apoptosis.**
*Cell Death and Disease* (2013) **4,** e940; doi:10.1038/cddis.2013.463; published online 5 December 2013
**Subject Category:** Cancer

The execution of apoptotic cell death is mediated by the caspase family of cysteine proteases. After being synthesized, caspases remain as inactive zymogens in the cell, where their activities are strictly regulated by protein–protein interactions and by proteolysis. Upon activation, caspases cleave each other's zymogens or other cellular substrates, thus eliciting orchestrated cellular destruction.[1,2] Among mammalian caspase family proteins, caspase-2 is the most conserved and evolutionarily related to CED-3, the *Caenorhabditis elegans* protease.[3,4] Yet, its biological function remains a matter of controversy. Over the past years, intense investigation of the function and activation mechanisms of caspase-2 has implicated this enzyme in stress-induced cell death pathways, including those triggered by DNA damage, microtubule destabilization and metabolic imbalance.[5–8] In addition, evidence for a potential role of caspase-2 in non-apoptotic pathways, including cell cycle regulation and DNA repair, is emerging (reviewed in Vakifahmetoglu-Norberg and Zhivotovsky[9] and Kumar[10]).

Caspase-2 possesses features of both initiator and executioner caspases. It shares sequence homology with the initiator caspases, especially caspase-9, but compared with other known caspases, which require tetrapeptide specificity for cleavage, the preferred substrate for caspase-2 is the pentapeptide VDVAD and the predicted substrate specificity of caspase-2 is more like that of caspase-3 or -7.[11–14] Among all cellular proteins that are known to be cleaved by caspases, only a few have been reported to serve as substrates for caspase-2. In addition to itself, active caspase-2 has been shown to cleave CUX-1, huntingtin (Htt), αII-spectrin, Bid, Rho kinases-2 (Rock-2), PKCδ, plakin, HDAC4, MDM-2, ICAD, PARP and DNp63a.[15–26] Most of these proteins are substrates for multiple proteases, including calpains and other caspases, and the functional consequences of their cleavage by caspase-2 remain unclear. The only caspase-2-specific substrate is the peripheral Golgi membrane protein golgin-160,[15] which possesses a caspase-2-specific cleavage site. In addition, desmoplakin, a cytoskeletal protein, has been reported to be subject to caspase-2 cleavage.[25] Although the

[1]Division of Toxicology, Institute of Environmental Medicine, Karolinska Institutet, Stockholm 171 77, Sweden; [2]National Institute for Infectious Diseases, IRCCS L Spallanzani, Rome 00149, Italy; [3]Department of Biological and Environmental Sciences and Technologies (DiSTeBA), University of Salento, Lecce 73100, Italy; [4]Department of Biology, University of Rome 'Tor Vergata', Rome 00173, Italy and [5]Lomonosov Moscow State University, Moscow 117192, Russia
*Corresponding authors: H Vakifahmetoglu-Norberg, Department of Cell Biology, Harvard Medical School, Boston, MA, USA. E-mail: Helin_Norberg@hms.harvard.edu. or B Zhivotovsky, Division of Toxicology, Institute of Environmental Medicine, Karolinska Institutet, Stockholm 171 77, Sweden. Tel: +46 852487588; Fax: +46 8329041; E-mail: Boris.Zhivotovsky@ki.se
[6]These authors contributed equally to this work.
[7]Present address: Department of Cell Biology, Harvard Medical School, Boston, MA, USA
[8]Present address: Department of Cancer Biology, Dana-Farber Cancer Institute, Boston, MA, USA
**Keywords:** apoptosis; caspase-2; cytoskeleton protein; protein degradation; proteomics
**Abbreviations:** Ac-DEVD-AMC, Ac-Asp-Glu-Val-Asp-AMC (AMC = 7-amino-4-methylcoumarin); Ac-VDVAD-AMC, Ac-Val-Asp-Val-Ala-Asp-AMC (AMC = 7-amino-4-methylcoumarin); BVA, biological variation analysis; 2D-DIGE, two-dimensional gel electrophoresis; DIA, differential in-gel analysis; Dox, doxorubicin; DTT, dithiothretiol; ER, endoplasmic reticulum; 5-FU, 5-fluorouracil; G3PDH, glyceraldehyde 3-phosphate dehydrogenase; GO, gene ontology; Htt, huntingtin; SDS-PAGE, sodium dodecyl sulfate-polyacrylamide gel electrophoresis; STS, staurosporine; UPS, ubiquitin–proteasome system; z-VDVAD-fmk, benzyloxycarbonyl-Val-Asp-Val-Ala-Asp-fluoromethyl ketone
Received 17.9.13; revised 23.10.13; accepted 24.10.13; Edited by A Stephanou

cleavage site and functional significance of this proteolysis are presently unknown, desmoplakin appears to be cleaved explicitly by caspase-2 and not by other caspases.

It seems likely that caspases might exert diverse functions based on their substrate selectivity during various cell fates. Whether caspase-2-mediated substrate cleavage is mandatory for apoptosis and which proteins it can cleave under different circumstances are yet to be determined. Therefore, the identification of novel caspase-2 substrates remains an important goal. In this study, we investigated the effect of active recombinant human caspase-2 on different subcellular compartments using a two-dimensional gel electrophoresis (2D-DIGE) proteomics approach. We used fractionated lysates of HCT116 human colon cancer cell line and compared the appearance or disappearance of protein peak intensities following treatment with recombinant caspase-2 alone or in combination with ankyrin (DARPin AR_F8), a specific caspase-2 inhibitor.[27] We found that the levels of four cytoskeleton proteins, tropomyosin, profilin, stathmin-1 and myotrophin, were decreased specifically in samples treated with recombinant caspase-2. The degradation profiles of these cytoskeleton proteins were further confirmed by western blotting in *in vitro* assays and during apoptotic signaling that requires caspase-2 activation. In samples where caspase-2 activity was pharmacologically inhibited, or downregulated using siRNA, the degradation of these proteins was blunted. Nonetheless, the degradation of the studied cytoskeleton proteins did not depend on the direct cleavage by caspase-2. Instead, caspase-2 probed these proteins for proteasomal degradation. Although the exact mechanism by which caspase-2 targets these proteins to the proteasome is unclear, our study suggests a novel role for caspase-2 in mediating proteasomal degradation of cytoskeleton proteins during apoptosis.

## Results

**Subcellular fractionation and optimization of conditions for recombinant caspase-2 activity.** To investigate whether any cytoskeleton proteins might serve as a caspase-2 substrate, we first fractionated HCT116 cells into cytosolic, membrane and nuclear compartments using the Qproteome Cell Compartment Kit (Figure 1a). Each of these fractions was separated on sodium dodecyl sulfate-polyacrylamide gel electrophoresis (SDS-PAGE), and proteins were visualized by Coomassie staining (Figure 1a). The purity of each fraction was verified by western blotting using antibodies against proteins known to reside in the respective compartments, including Lamin B (nucleus), glyceraldehyde 3-phosphate dehydrogenase (G3PDH) (cytosol) and cytochrome *c* (mitochondria) (Figure 1a). As the focus of this study was on cytoskeleton proteins, we continued our analysis using the cytosolic fraction and used an *in vitro* system consisting of active recombinant caspase-2 that was incubated with cytosolic HCT116 cell lysates. A fluorometric analysis using fluorogenic substrate, Ac-VDVAD-AMC (Ac-Val-Asp-Val-Ala-Asp-AMC (AMC = 7-amino-4-methyl-coumarin)), for caspase-2 was performed to verify the

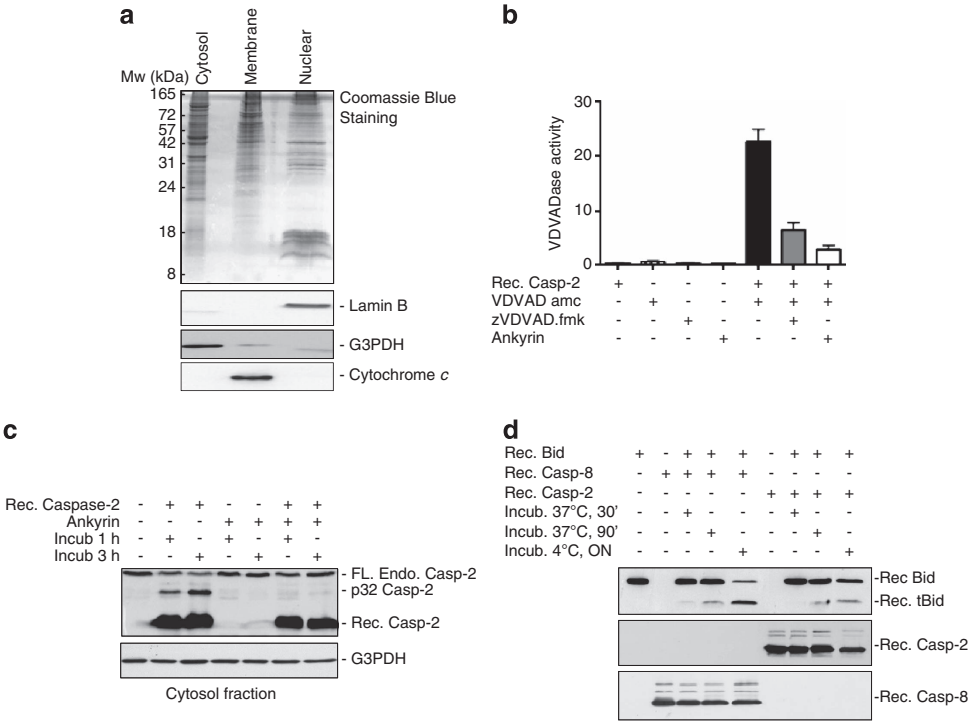


**Figure 1** Subcellular fractionation and optimization of conditions for recombinant caspase-2 activity. (**a**) Coomassie blue-stained gel showing separation of proteins in the different subcellular fractions of HCT116 cells. Western blots reveal the distribution of lamin B, G3PDH and cytochrome *c* between the cytosolic, membrane and nuclear fractions. (**b**) *In vitro* activity measurement of recombinant caspase-2 indicated by VDVAD-AMC release, in the absence or presence of either zVDVAD.fmk or ankyrin. Results are mean ± S.E. ($n = 3$). (**c**) Western blot showing the processing of endogenous caspase-2 in the cytosolic fraction of HCT116 cells. G3PDH antibody was used as a loading control. (**d**) Western blots showing Bid cleavage by recombinant caspase-2 or -8, at indicated time points and incubation (Incub.) conditions. ON, overnight

activity of recombinant caspase-2 in this context (Figure 1b). The caspase-2 substrate, Ac-VDVAD-AMC and inhibitors, z-VDVAD-fmk (benzyloxycarbonyl-Val-Asp-Val-Ala-Asp-fluoromethyl ketone) or ankyrin, were included in selected samples as indicated (Figure 1b). The results revealed a high activity of recombinant caspase-2 as a pronounced increase in Ac-VDVAD-AMC cleavage was observed (Figure 1b), which was inhibited by VDVAD-fmk or ankyrin. Furthermore, the ability of recombinant caspase-2 to cleave its precursor, endogenous caspase-2, was tested in digitonin-permeabilized HCT116 cells. Addition of recombinant caspase-2 to cells led to a marked processing of endogenous caspase-2 in a time-dependent manner, which was blocked by ankyrin (Figure 1c). To further confirm the activity of recombinant caspase-2, the *in vitro* cleavage of its known substrate Bid into truncated tBid was tested. Recombinant Bid was mixed with either recombinant caspase-2 or recombinant caspase-8 (positive control) for various time periods and temperatures. As seen in Figure 1d, formation of tBid occurred in a time-dependent manner using caspase-2 as well as caspase-8.

**Active recombinant caspase-2 in cellular lysates does not trigger effector caspase cascades.** Caspase-2 is known to not cleave, or proteolytically activate, executioner caspases under physiological conditions.[28] Hence, to exclude the possibility that the presence of active recombinant caspase-2 may lead to the activation of downstream effector caspases that could cleave additional proteins in the cell lysates, we examined the processing of caspase-3 and -7, as well as the activities of these caspases in recombinant caspase-2-treated cytosol fractions. Western blot analysis of these lysates revealed processing of endogenous caspase-2, whereas processing of endogenous caspase-3 or -7 was not detected (Figure 2a). This observation was further corroborated when recombinant active caspase-2 was incubated with HCT116 cytosolic fractions in the presence/absence of either the caspase-2 substrate (Ac-VDVAD-AMC) or caspase-3 and -7 substrate (Ac-DEVD-AMC (Ac-Asp-Glu-Val-Asp-AMC (AMC = 7-amino-4-methylcoumarin))). Results from the fluorometric analysis illustrated a high VDVADase activity of caspase-2, whereas no caspase-3/-7 DEVDase activity was detected (Figure 2b). DEVDase activity could only be detected in samples treated with active recombinant caspase-3. These data demonstrate that active recombinant caspase-2 did not activate downstream effector caspases in the experimental settings used in this study.

**Proteomic analysis reveals potential caspase-2 substrates.** Next, we used a differential proteome analysis using 2D-DIGE on HCT116 cytosolic fractions (Figure 3a). Equal amounts of cytosolic fractions were treated with purified recombinant active caspase-2 alone or in combination with ankyrin. To do that three independent sample groups labeled with either Cy3 or Cy5 dyes were used for evaluation of the protein profiles in multiple samples simultaneously. The same amount of internal standard was labeled with Cy2. Differentially labeled samples were mixed and the protein content was subsequently separated, first according to pH followed by size. Scanned gel images of separated proteins were analyzed using the DeCyder2D 6.5 Differential analysis software (GE Healthcare, Little Chalfont, Buckinghamshire, UK). Differential in-gel analysis (DIA) and biological variation analysis (BVA) were performed for an intra- and intergel statistical analysis, to provide relative

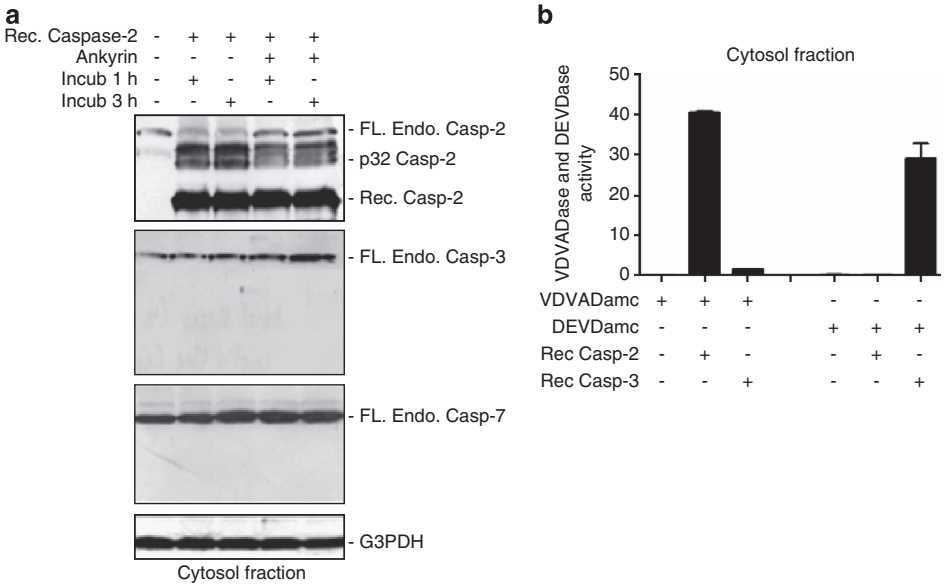


**Figure 2** Effector caspases are not activated by recombinant caspase-2 in cellular lysates. (**a**) Western blot showing the processing of endogenous caspase-2 and the absence of endogenous caspase-3 and caspase-7 processing in recombinant caspase-2-treated cytosolic fraction of HCT116 cells for indicated incubation (Incub.) times. Western blots of caspase-2, -3 and -7 processing. G3PDH antibody was used as a loading control. (**b**) Caspase activity assay shows the activities of caspase-2 and caspase-3/-7 in cytosolic fraction isolated from HCT116 cells. VDVAD-AMC, fold increase in caspase-2 activity; DEVD-AMC, fold increase in caspase-3/-7-like activity. Results are mean ± S.E. ($n = 3$)

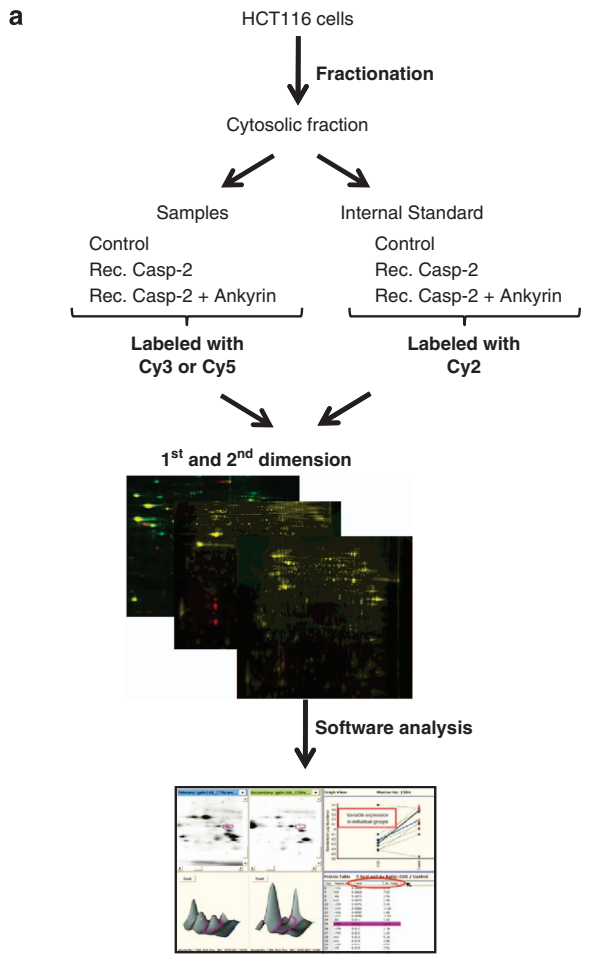


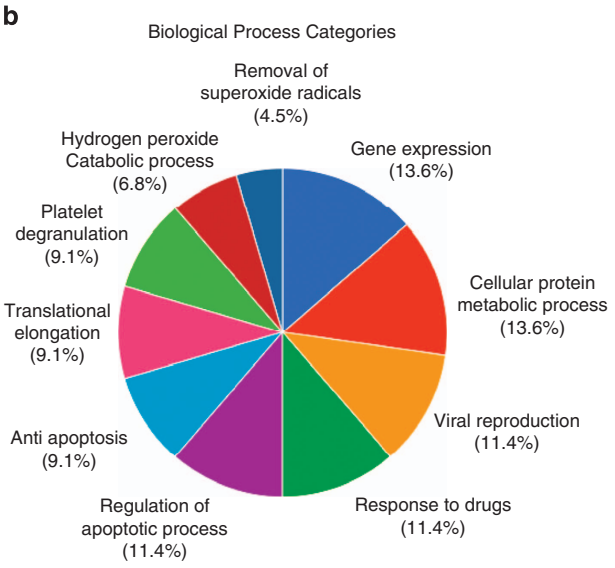


**c**

| | Gene name | Description | Fold change Casp-2/Ctrl | Fold change Ctrl/ (Casp-2+Ankyrin) | P-value (t-test) Casp-2/Ctrl | P-value (t-test) Ctrl/ (Casp-2+Ankyrin) |
|---|---|---|---|---|---|---|
| 1 | SOD1 | superoxide dismutase 1, soluble | -3.82 | 1.15 | 0.0007 | 0.0078 |
| 2 | FABP5 | fatty acid binding protein 5 | -2.82 | 1.05 | 0.0008 | 0.0087 |
| 3 | TXN | thioredoxin | -2.81 | 0.99 | 0.0016 | 0.0120 |
| 4 | PPIA | peptidylprolyl isomerase A (cyclophilin A) | -2.72 | 1.10 | 0.0041 | 0.0140 |
| 5 | PRPF31 | PRP31 pre-mRNA processing factor 31 homolog | -1.89 | 1.01 | 0.0042 | 0.0160 |
| 6 | TPM3 | tropomyosin 3 | -3.15 | 1.12 | 0.0048 | 0.0170 |
| 7 | STMN1 | stathmin 1 | -2.86 | 1.09 | 0.0064 | 0.0190 |
| 8 | MTPN | myotrophin | -2.72 | 1.02 | 0.0069 | 0.0220 |
| 9 | TPM2 | tropomyosin 2 (beta) | -1.93 | 1.05 | 0.0077 | 0.0230 |
| 10 | PFN1 | profilin 1 | -2.54 | 0.99 | 0.0079 | 0.0260 |

**Figure 3** Identification of cytosolic proteins affected by recombinant caspase-2 activity. (**a**) Schematic presentation and performance of the 2D-DIGE assay. (**b**) The categorization of all identified proteins according to the biological process using singular enrichment analysis. (**c**) The list of potential cytosolic proteins affected by recombinant caspase-2 activity

abundance in the various groups. The abundant protein ratios were subsequently compared between control and caspase-2-treated samples from all three gels using the statistical analysis. By this method, we were able to identify 38 protein peaks that were less abundant in the samples treated with recombinant caspase-2 compared with that of untreated controls. These proteins were identified by MALDI-MS and MALDI-MS/MS, and recorded MS spectra were searched by Mascot algorithm among human proteins in the Swiss-Prot database (see full list in Table 1). Notably, several of the proteins identified in this list overlap and are similar to some of the reported proteins that harbor caspase-2 cleavage sites by degradomics data.[29] To gain further insight into the identified protein hits, bioinformatic analysis was performed. The identified proteins were categorized according to singular enrichment analysis of biological process. Gene ontology (GO) showed a highly significant enrichment of proteins involved in gene expression, metabolic processes and viral reproduction (Figure 3b). The results of GO biological process analysis also showed significant enrichment of proteins involved in drug response and regulation of the apoptotic process. The latter findings

**Table 1** The list of caspase-2-affected proteins identified by 2D-DIGE proteomics approach in cytosolic fraction of HCT116

| Gene name | Protein description |
|---|---|
| *SOD1* | Superoxide dismutase 1, soluble |
| *FABP5* | Fatty acid-binding protein 5 (psoriasis-associated) |
| *TXN* | Thioredoxin |
| *PPIA* | Peptidylprolyl isomerase A (cyclophilin A) |
| *PRPF31* | PRP31 pre-mRNA processing factor 31 homolog (*S. cerevisiae*) |
| *SF3A3* | Splicing factor 3a, subunit 3, 60 kDa |
| *ACTG1* | Actin, $\gamma$1 |
| *EIF6* | Eukaryotic translation initiation factor 6 |
| *TPM3* | Tropomyosin 3 |
| *STMN1* | Stathmin 1 |
| *CFL1* | Cofilin 1 (non-muscle) |
| *TBCA* | Tubulin folding cofactor A |
| *MTPN* | Myotrophin |
| *TPM2* | Tropomyosin 2 ($\beta$) |
| *PFN1* | Profilin 1 |
| *PRDX1* | Peroxiredoxin 1 |
| *PRDX2* | Peroxiredoxin 2 |
| *PRDX6* | Peroxiredoxin 6 |
| *PARK7* | Parkinson protein 7 |
| *EIF5A* | Eukaryotic translation initiation factor 5A |
| *EEF1A1* | Eukaryotic translation elongation factor 1$\alpha$1 |
| *EIF1AX* | Eukaryotic translation initiation factor 1A, X-linked |
| *RPS12* | Ribosomal protein s12 |
| *RPS17* | Ribosomal protein s17 |
| *SKP1* | S-phase kinase-associated protein 1 |
| *LGALS1* | Lectin, galactoside-binding, soluble, 1 |
| *MIF* | Macrophage migration inhibitory factor (symbol; acc: 7097) |
| *DNAJC8* | DNAJ (HSP40) homolog, subfamily C, member 8 |
| *RANBP1* | RAN-binding protein 1 |
| *PPP1R1A* | Protein phosphatase 1, regulatory (inhibitor) subunit 1A |
| *PEBP1* | Phosphatidylethanolamine-binding protein 1 |
| *CSTB* | Cystatin B (stefin B) |
| *TPT1* | Tumor protein, translationally controlled 1 |
| *NME1* | Non-metastatic cells 1, protein (NM23A) |
| *TPI1* | Triosephosphate isomerase 1 |
| *CRABP1* | Cellular retinoic acid-binding protein 1 |
| *UBE2N* | Ubiquitin-conjugating enzyme E2N |
| *SET* | Set nuclear oncogene |

confirm an important role for caspase-2 in the regulation of apoptosis.

Next, we compared the peak intensities of the identified proteins in samples treated with caspase-2 alone to those cotreated with caspase-2 and the caspase-2 inhibitor, ankyrin. This allowed us to identify unambiguously proteins that were degraded only in the presence of active caspase-2. Out of 38 proteins, we found a total of 10 proteins that were no longer degraded in the presence of ankyrin (listed in Figure 3c). Fifty percent of these 10 proteins were identified as cytoskeleton proteins, the levels of which were changed with high ratio values, including tropomyosin, myotrophin, profilin and stathmin-1.

**Degradation of identified cytoskeleton proteins is dependent on caspase-2 activation during apoptosis.** As a validation of the identified cytoskeleton proteins, we verified their degradation status by western blotting upon incubation of HCT116 cytosolic fraction with recombinant caspase-2 (Figure 4a). Although the protein levels of tropomyosin, myotrophin, profilin and stathmin-1 were all decreased by active recombinant caspase-2 treatment, cotreatment with ankyrin attenuated caspase-2-induced degradation of these cytoskeleton proteins, which further confirmed our observation using 2D-DIGE (Figure 4a).

We have previously shown that DNA damage induces caspase-2 activation in HCT116 cells.[8,30] Thus, in addition to the *in vitro* assay used, we examined whether the identified cytoskeleton protein levels were also affected during apoptosis. HCT116 cells were treated with three different apoptotic stimuli, 5-fluorouracil (5-FU), doxorubicin (Dox) and staurosporine (STS), to determine the best condition in which HCT116 cells underwent apoptotic cell death with significant caspase-2 processing and activity (Figure 4b). In selected samples, cells were incubated with z-VDVAD-fmk for 1 h before treatment with the proapoptotic agents. Caspase-2 activity was measured by the VDVADase cleavage assay, and its processing was visualized by western blotting. As shown in Figure 4b, caspase-2 had the highest activity after treatment with 5-FU, and approximately 70% of its activity was inhibited in the presence of z-VDVAD-fmk. In addition, a pronounced caspase-2 processing was seen after treatment with 5-FU, whereas Dox or STS treatments led to a lesser increase of the 32 kDa fragment of processed caspase-2 (Figure 4b). Further, the protein levels of tropomyosin, myotrophin, profilin and stathmin-1 were decreased upon 5-FU exposure in a time-dependent manner, concurrently with caspase-2 processing (Figure 4c) and when significant caspase-2-mediated apoptosis was detected (Figure 4d). Importantly, the observed decrease in cytoskeleton protein levels and processing of caspase-2 as well as apoptotic cell death were inhibited by z-VDVAD-fmk (Figures 4c and d), which demonstrated the importance of caspase-2 for the observed decrease in the levels of cytoskeleton proteins. To substantiate these findings, we utilized a genetic approach, using siRNA targeting of caspase-2 (Figure 4e) and found that silencing of caspase-2 blunted the degradation of profilin, stathmin-1, myotrophin and tropomyosin in 5-FU-treated cells (Figure 4f). Taken together, both genetic and pharmacological approaches support the notion that caspase-2 is required for the observed decrease in the levels of tropomyosin, myotrophin, profilin and stathmin during caspase-2-mediated apoptotic cell death.

Next, we investigated the effect of apoptotic stimuli other than DNA damage on the protein levels of tropomyosin, myotrophin, profilin and stathmin-1. We used paclitaxel that is a microtubule-stabilizing agent, which has previously been shown to induce cell death that is significantly inhibited in *Casp2*$^{-/-}$ mouse embryonic fibroblasts.[6] In addition, we tested the effect of thapsigargin and tunicamycin, two agents that lead to endoplasmic reticulum (ER) stress-induced cell death, in which caspase-2 has been demonstrated to have a significant role. As shown in Figure 4g, treatment of HCT116 cells with paclitaxel, thapsigargin or tunicamycin led to a pronounced decrease in the levels of cytoskeleton protein. Degradation of tropomyosin, myotrophin, profilin and stathmin-1 was also observed using SUM159, a breast carcinoma cell line upon treatment with paclitaxel and tunicamycin (Figure 4h). In both cell lines tested, degradation of these cytoskeleton proteins was inhibited in the presence of z-VDVAD-fmk, demonstrating the extensiveness of the degradation effect of these proteins during apoptotic cell death and implicating the role for caspase-2 in the mediation of their degradation.

**Caspase-2 targets cytoskeleton proteins for proteasomal degradation.** To investigate whether the observed degradation of cytoskeleton proteins was due to their direct cleavage by caspase-2, we expressed and purified recombinant stathmin, myotrophin, tropomyosin and profilin using immobilized metal affinity chromatography. *In vitro* cleavage assay was performed, in which a previously known caspase-2 substrate Bid was initially incubated with

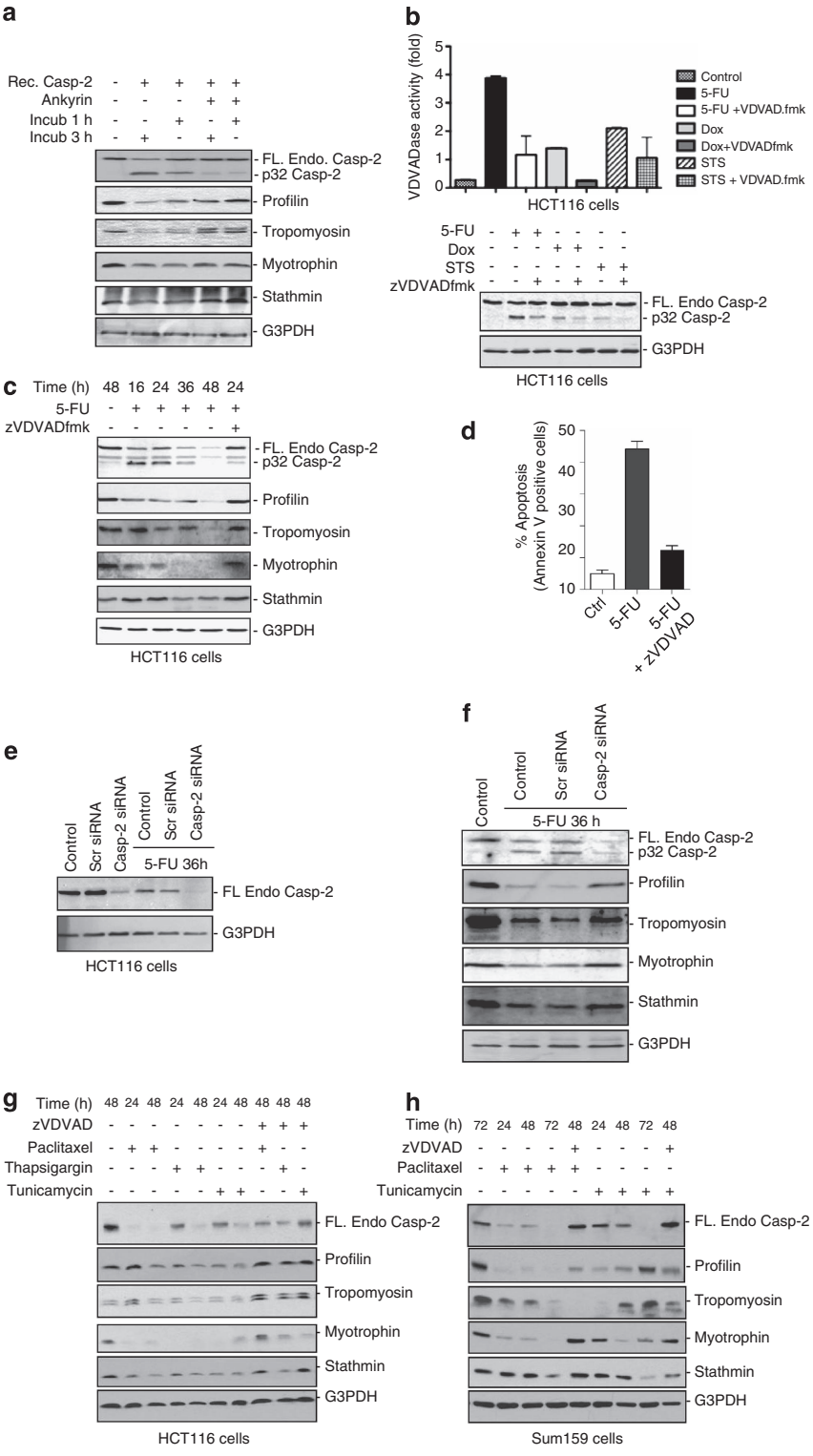

recombinant caspase-2 as a positive control (Figure 5a). The results revealed that under these experimental conditions, caspase-2 can potently cleave Bid, and that this cleavage can be prevented by ankyrin (Figure 5a). Next, recombinant profilin, tropomyosin, stathmin and myotrophin were incubated for different time periods under the same conditions as used for Bid (Figure 5b). The obtained results were negative and implicated that the effect of caspase-2 on the levels of the cytoskeleton proteins in apoptotic cells was not dependent on their direct cleavage of caspase-2. Recombinant active caspase-3 was also tested on selected samples; however, the studied cytoskeleton proteins were not directly cleaved by caspase-3 either (Figure 5b). To exclude the possibility that the antibodies used in western blotting may not have recognized potential cleavage products of these cytoskeleton proteins, profilin, tropomyosin, stathmin and myotrophin were radiolabeled using [$^{35}$S]methionine TNT-coupled reticulocyte lysate system, and were incubated with recombinant caspase-2. However, no cleavage products of these proteins were detected (Figure 5c). Therefore, we conclude that the degradation of these cytoskeleton proteins during caspase-2-mediated apoptosis is not the result of their direct cleavage by caspase-2.

To further investigate the pathway by which caspase-2 activity can trigger the degradation of cytoskeleton proteins, we took advantage of inhibitors of the proteasomal degradation pathway. Pretreatment of cells with either MG132 or bortezomib (Velcade), two well-known proteasomal inhibitors, reversed the caspase-2-dependent degradation of profilin, myotrophin, stathmin and tropomyosin and led to their accumulation in 5-FU-treated HCT116 cells (Figure 5d). We could further confirm that application of inhibitor that blocks calpains (PD150606) has negligible effect on 5-FU-mediated cytoskeleton protein degradation (Figure 5e).

Next, we investigated the susceptibility of these proteins to ubiquitination. Consistent with their degradation via the proteasome, 5-FU treatment led to the accumulation of ubiquitinated profilin, myotrophin, stathmin and tropomyosin in HCT116 cells. The augmented ubiquitination status was not observed in samples treated with caspase-2 inhibitor, further confirming that these proteins were targeted for proteasomal degradation during apoptosis in a caspase-2-dependent manner (Figure 5f).

## Discussion

While previous reports demonstrate a link between caspase-2 activation and cytoskeletal protein disruption,[6,31] we present here the identification of several potential caspase-2 targets among cytoskeletal proteins during apoptotic cell death. Using 2D-DIGE proteomics approach followed by mass spectrometric analysis, we have identified tropomyosin, myotrophin, profilin and stathmin-1 as four cytoskeleton proteins that were specifically targeted by recombinant caspase-2 *in vitro*. Degradation of these proteins appeared to occur in a time-dependent manner following caspase-2 activation during apoptotic signaling induced by DNA damage, ER stress or cytoskeleton disruption, whereas inhibition of caspase-2 activity, or genetic silencing of caspase-2, prevented their degradation. Thus, our study proposes a role for caspase-2 in the regulation of the level of cytoskeleton proteins during apoptosis.

Although we used a direct approach by adding active recombinant caspase-2 to either cell lysates or recombinant or radiolabeled proteins, we were unable to detect a cleaved product of the identified cytoskeletal proteins, suggesting that their degradation is independent of their direct cleavage mediated by caspase-2. Instead, we discovered a functional link between caspase-2 and the degradation of cytoskeleton proteins via the ubiquitin–proteasome system (UPS). Application of compounds that inhibit proteasomes but not calpains blocks the degradation of the studied cytoskeleton proteins. Several potential mechanisms may account for the effect of caspase-2 in probing these cytoskeleton proteins for proteasomal degradation. Caspase-2 might activate cellular proteins or processes that facilitate cytoskeleton degradation/disruption. Major degradation systems, including UPS, have been suggested to be activated by inactivation of the Rho GTPase effector, Rock-2, that has central roles in the organization of the actin cytoskeleton, which has previously shown to be cleaved by caspase-2.[32] It is also likely that deubiquitination enzymes, which regulate the stability of cytoskeletal proteins, may act as downstream targets of caspase-2, which when cleaved lead to constitutive ubiquitination of its substrates. Another possibility is that proteins essential for cytoskeleton polymerization and/or stabilization are targeted and may be cleaved by caspase-2 during apoptosis, leading to destabilization and degradation of the cytoskeleton filaments. In fact, intermediate filament protein, such as vimentin, cytolinker

**Figure 4** Caspase-2 is required for the degradation of the identified cytoskeleton proteins. (**a**) Western blots showing the *in vitro* protein levels of profilin, tropomyosin, myotrophin and stathmin, as well as processing of endogenous caspase-2 in HCT116 cytosolic fraction treated with recombinant caspase-2 at indicated time points in the presence or absence of ankyrin. G3PDH antibody was used as a loading control. (**b**) *In vitro* VDVADase activity, indicated by VDVAD-AMC release, in HCT116 cells treated by 5-FU, Dox or STS in the absence or presence of zVDVAD.fmk. Results are mean ± S.E. (Lower panel) Western blot of caspase-2 showing the processing into the 32 kDa fragment in HCT116 cells in response to treatment with 5-FU, Dox and STS in the presence and absence of z-VDVAD-fmk. (**c**) Western blot determination of a time-dependent decrease of profilin, tropomyosin, myotrophin and stathmin protein levels in HCT116 cells following 5-FU treatment in the presence or absence of z-VDVAD-fmk. Caspase-2 processing is shown, indicated by the 32 kDa fragment. (**d**) Annexin V-positive apoptotic HCT116 cells upon 5-FU treatment, in the absence and presence of zVDVAD.fmk, detected by FACS analysis. (**e**) Western blots showing the efficiency of caspase-2 siRNA in untreated and 5-FU-treated HCT116 cells. (**f**) Western blots showing the protective effect of caspase-2 silencing on the degradation of profilin, tropomyosin, stathmin and myotrophin. The scrambled (Scr) siRNA was used as a negative control. (**g**) Determination of a time-dependent decrease of profilin, tropomyosin, myotrophin and stathmin protein levels in HCT116 cells following treatment with paclitaxel, thapsigargin or tunicamycin in the presence or absence of z-VDVAD-fmk. Caspase-2 processing is shown by the disappearance of the full-length fragment. (**h**) Western blots showing a time-dependent decrease of profilin, tropomyosin, myotrophin and stathmin protein levels in SUM159 cells following treatment with paclitaxel and tunicamycin in the presence or absence of z-VDVAD-fmk. Caspase-2 processing is shown by the disappearance of the full-length fragment. G3PDH was used for control of equal loading in all western blots

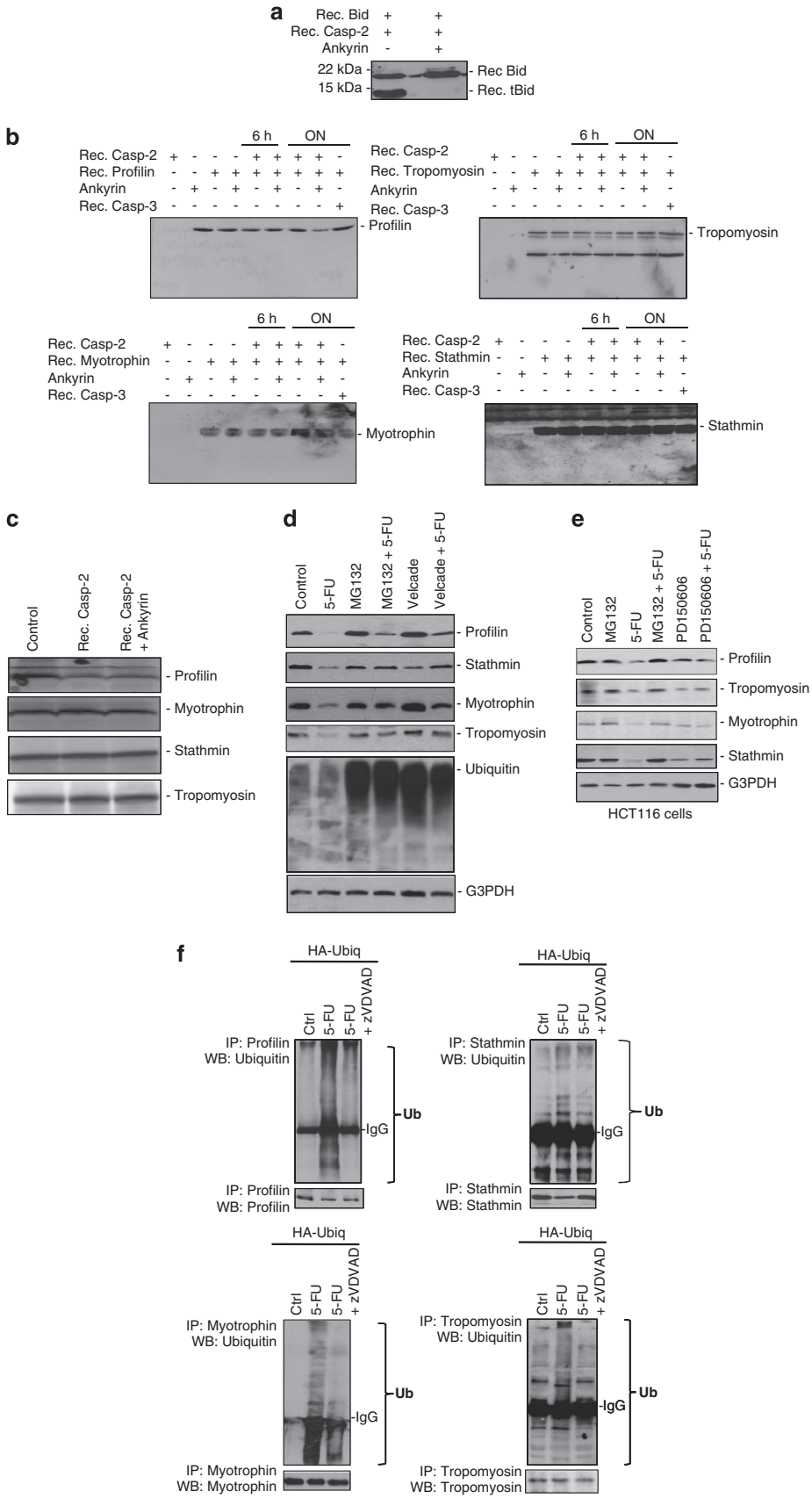
a
Rec. Bid
Rec. Casp-2
Ankyrin
22 kDa
15 kDa
Rec Bid
Rec. tBid
b
6 h
ON
Rec. Casp-2
Rec. Profilin
Ankyrin
Rec. Casp-3
Profilin
Rec. Tropomyosin
Tropomyosin
Rec. Myotrophin
Myotrophin
Rec. Stathmin
Stathmin
c
Control
Rec. Casp-2
Rec. Casp-2 + Ankyrin
Profilin
Myotrophin
Stathmin
Tropomyosin
d
Control
5-FU
MG132
MG132 + 5-FU
Velcade
Velcade + 5-FU
Profilin
Stathmin
Myotrophin
Tropomyosin
Ubiquitin
G3PDH
e
Control
MG132
5-FU
MG132 + 5-FU
PD150606
PD150606 + 5-FU
Profilin
Tropomyosin
Myotrophin
Stathmin
G3PDH
HCT116 cells
f
HA-Ubiq
Ctrl
5-FU
5-FU + zVDVAD
IP: Profilin
WB: Ubiquitin
IgG
Ub
IP: Profilin
WB: Profilin
IP: Stathmin
WB: Ubiquitin
IP: Stathmin
WB: Stathmin
IP: Myotrophin
WB: Ubiquitin
IP: Myotrophin
WB: Myotrophin
IP: Tropomyosin
WB: Ubiquitin
IP: Tropomyosin
WB: Tropomyosin

protein plectin, actin-binding proteins gelsolin, HS1, cortactin and HIP-55 have been demonstrated to be caspase substrates during apoptosis.[33,34] However, whether these linker and stabilizer proteins are cleaved by caspase-2 remains to be investigated.

The marked morphological changes in apoptotic cells include a complete reorganization of the cytoskeleton. The cytoskeleton is involved in various steps of the apoptotic process; in particular, the cleavage of several cytoskeleton components by caspases ensures a rapid and organized breakdown of the cell into apoptotic bodies. Profilin is an actin-binding protein that has a crucial role in regulating actin polymerization. Interestingly, profilin directly interacts with Htt, a well-known caspase-2 substrate,[22] whereas the expression of mutant Htt enhances degradation of profilin and thus alters the ratio of polymerized to unpolymerized actin.[35] The increased profilin turnover observed with mutant Htt is suggested to be a result of decreased interaction between wt Htt and profilin, which indicates that the stability of profilin is dependent on the interaction to its binding partners.[35] It is, therefore, possible that the proteolytic cleavage of Htt by caspase-2 could cause profilin dissociation from Htt and subsequent degradation through UPS.

Stathmin is an ubiquitous cytosolic phosphoprotein that regulates the polymerization of microtubules. In its unphosphorylated form, stathmin promotes depolymerization of microtubules and enhances microtubule dynamics. Notably, PUMA overexpression due to p53 activation has been shown to induce stathmin degradation through a proteasome-mediated mechanism, which leads to disruption of the cellular microtubule network in apoptotic cells.[36] As p53 expression is fundamental for caspase-2 activation during 5-FU-mediated cell death in HCT116 cells,[8] these data further support our findings indicating a crucial role of caspase-2 in regulating stathmin levels and thereby cellular microtubule network in apoptotic cells.

Tropomyosin, which is also an actin-binding protein, forms continuous polymers along the major groove of actin filaments. It stabilizes actin filament and has a role in actin dynamics. Myotrophin is the smallest known ankyrin repeat protein, and it promotes the polymerization of actin by binding the capping protein. Thereby, all of these proteins are associated with actin or tubulin filaments, and have the essential regulatory function in stabilizing the integrity of cytoskeleton. It is most likely that their degradation leads to the loss of their function, leading to reorganization and destabilization of actin filaments, essential for the apoptosis-related morphological changes. Beyond the specific degradation process, it is, however, still unclear whether the disruption of these cytoskeleton proteins is an amplifying step for the apoptotic process or if their degradation is consequence of apoptosis.

Altogether, our findings suggest that the regulation of the stability of multiple cytoskeleton proteins is mediated by caspase-2. Although the exact mechanisms as to how caspase-2 activation mediates the ubiquitination and subsequent degradation of these proteins remain to be investigated further, our data support the notion that targeting the cytoskeleton by activating caspase-2 might increase the efficiency of cancer treatment, as actin-binding proteins, fundamental for regulating the dynamics of actin polymerization, have been implicated to have determinant roles in cancer transformation and metastasis.

## Materials and Methods

**Cell culture.** The parental HCT116 human colon cancer cell line was cultured in DMEM complete medium supplemented with 10% (v/v) heat-inactivated fetal bovine serum, L-glutamine (2 mM), penicillin (100 U/ml) and streptomycin (100 $\mu$g/ml) in a humidified 5% $CO_2$ atmosphere at 37 °C. The SUM159 breast cancer cell line was cultured in Ham's F12 (5% FBS, 1% penicillin/streptomycin, insulin (5 mg/ml) and hydrocortisone (2 mg/ml)). Cells were maintained in logarithmic growth phase for all experiments. Cell culture medium and supplements were purchased from Invitrogen (Stockholm, Sweden), unless otherwise stated. Cells were exposed to 375 $\mu$M 5-FU, 1.2 $\mu$g/$\mu$l Dox, 0.2 $\mu$M STS, 100 $\mu$M paclitaxel, 1 $\mu$M thapsigargin or 1.5 $\mu$M tunicamycin as described before[6,8,37] to induce cell death. In selected experiments, equal amounts of protein from cell extracts/fractions were treated with purified recombinant active caspase-2 (1.2 $\mu$g/ml) alone or in combination with the caspase-2 inhibitor and ankyrin repeat protein (6 $\mu$g/ml). In selected experiments, the caspase-2 inhibitor z-VDVAD-fmk (20 $\mu$M) and the caspase-3 inhibitor z-DEVD-fmk (10 $\mu$M) (Enzyme Systems Products, Livermore, CA, USA) were added to the cells 1 h before treatment with 5-FU. In some experiments, MG132 (2 $\mu$M), Velcade (bortezomib 0.1–1 $\mu$M) or the calpain inhibitor PD150606 (150 $\mu$M) were used.

***In vitro* reaction with caspase-2.** Equal amounts of protein from each sample were diluted with Tris-caspase-2 reaction buffer containing 1 mM dithiothretiol (DTT) up to 600 $\mu$l reaction volume. Purified recombinant active caspase-2 (1.2 $\mu$g/ml) was either added to each fraction sample alone or in combination with ankyrin (6 $\mu$g/ml). Samples were incubated for 4 or 6 h, or overnight at 37 °C. The reaction was terminated by acetone precipitations of the proteins or by adding 5 $\times$ Laemmli's loading buffer (62.5 mM Tris-HCl (pH 6.8), 5% $\beta$-mercaptoethanol, 2% SDS, 10% glycerol and 0.002% bromophenol blue) for 2D-DIGE or western blot analysis, respectively.

**Sample preparation and 2D-DIGE analysis.** Cytosolic proteins were isolated from HCT116 cells using Qproteome Cell Compartment Kit (Qiagen, Hilden, Germany) according to the manufacturer's instruction. The isolation was followed by the determination of protein concentration using the BSA assay (Pierce, Rockford, IL, USA) and fractionation assessed by western blotting. Cytosolic proteins were precipitated and cleaned using ETTAN 2D Clean-Up Kit (GE Healthcare) according to the manufacturer's instructions, and dissolved in sample buffer (7 M urea, 2 M thiourea, 2% CHAPS, 1% sulfobetaine 3–10, 1% amidosulfobetaine14 and 10 mMTris-HCl (pH8.5)). 2D-DIGE analysis relies on the prelabeling of protein samples with two fluorescently resolvable dyes, which are mixed and run together with an internal standard labeled with a third dye. The internal standard is used to match spots across a gel series and to calculate standardized abundances. Fifty micrograms of cytosolic proteins were labeled with 200 pmol of the *N*-hydroxy succinimidyl ester derivatives of the cyanine dyes Cy3 or Cy5 according to the manufacturer's instructions (GE Healthcare). Same amount of internal standard was labeled with Cy2. Differentially labeled samples

**Figure 5** Caspase-2 targets cytoskeleton proteins to the proteasome. (**a**) *In vitro* cleavage of recombinant Bid by recombinant caspase-2. (**b**) *In vitro* cleavage assay of recombinant profilin, tropomyosin, myotrophin and stathmin incubated with recombinant active caspase-2 or caspase-3 at indicated time points and conditions. (**c**) *In vitro* cleavage assay of radiolabeled profilin, tropomyosin, myotrophin and stathmin incubated with recombinant active caspase-2, in the presence or absence of ankyrin. ON, overnight. (**d**), Western blots showing the levels of profilin, tropomyosin, myotrophin and stathmin in the presence or absence of the proteasome inhibitors, MG132 and Velcade (Bortezomib), or (**e**) calpain inhibitor, PD150606, following 5-FU treatment of HCT116 cells. G3PDH was used for control of equal loading. (**f**) HA-ubiquitin-transfected HCT116 cells (24 h), pretreated with MG132 (30 min), were treated with 5-FU in the presence or absence of zVDVAD.fmk for 24 h. Cell lysates were subject to immunoprecipitation using antibody against profilin, stathmin, tropomyosin and myotrophin, followed by ubiquitin western blot

were mixed together and supplemented with equal amount of urea buffer, containing DTT (20 mg/ml) and ampholines, pH 3–10 (2% (v/v). A dye-swapping scheme was used to ensure that samples from both groups were labeled either with Cy3 or with Cy5, and each gel contained one sample from each group. Proteins were subjected to IEF using nonlinear 3–10 pH range dry strips on a IPGphor II (GE Healthcare) according to the manufacturer's instructions. Second dimension electrophoresis was performed on 12% polyacrylamide gels at 8 mA/gel for 16 h in Tris-glycine SDS-PAGE running buffer (Bio-Rad, Hercules, CA, USA).

**Image analysis.** The Cy2-, Cy3- and Cy5-labeled images were acquired on a Typhoon 9410 scanner (GE Healthcare). Gels were then fixed in 10% (v/v) methanol and 7% (v/v) acetic acid and stained with SyproRuby (Bio-Rad). Images were imported in DeCyder v.6.5, 2D Differential Analysis Software (GE Healthcare). The DeCyder DIA software was used for spot codetection and normalized volume ratio calculation. DeCyder BVA software was then used to match simultaneously all spot maps from 2D-DIGEs and to identify spots with statistical variations using the Student's *t*-test.

**Protein excision and tryptic digestion.** Selected spots were excised from the gels using a software-driven ProPic Spot picker (Genomic Solutions, Ann Arbor, MI, USA) and subjected to in-gel tryptic digestion. Briefly, gel pieces were washed two times in 100 mM ammonium bicarbonate and 50% (v/v) ACN, dehydrated by incubation in 100% (v/v) ACN for 5 min and rehydrated in 50 mM ammonium bicarbonate containing 4 ng/$\mu$l of trypsin. Rehydratation was allowed for 30 min, the excess of trypsin was discharged and 50 mM ammonium bicarbonate was added following digestion overnight at 37 °C. Peptides in solution were conserved at $-20$ °C until analysis.

**Protein identification by MALDI-MS and MS/MS.** Tryptic peptides were concentrated with ZipTip mC18 pipette tips (Millipore, Billerica, MA, USA) and coeluted onto the MALDI target in 1 $\mu$l of $\alpha$-cyano-4-hydroxycinnamic acid matrix (5 mg/ml in 50% ACN, 0.1% TFA). MALDI-MS and MALDI-MS/MS were performed on an Applied Biosystems 4700 Proteomics Analyzer (AB Sciex, Framingham, MA, USA) with TOF/TOF ion optics as described.[38] Calibration was performed using peptides resulting from autoproteolysis of trypsin (*m/z*: 842.510, 1045.564, 2211.105, 2239.136 and 2807.300). In addition to peptide mass finger spectra, the five most abundant precursor ion masses having an S/N $>50$ were chosen for MS/MS fragmentation. The interpretation of both the MS and MS/MS data were carried out with the GPS Explorer software (Version 3.6; AB Sciex). An exclusion list of known contaminant ion masses of keratin and trypsin (842.510, 906.505, 917.300, 947.500, 1045.564, 1794.810, 2211.105, 2239.136, 2283.181, 2284.184 and 2300.178) was used. A combined MS peptide fingerprint and MS/MS peptide sequencing search was performed against the NCBI human database using the MASCOT search algorithm. These searches specified trypsin as the digestion enzyme, carbamidomethylation of cysteine as fixed modification, partial oxidation of methionine and allowed for one missed trypsin cleavage. The monoisotopic precursor ion tolerance was set to 30–70 p.p.m. and the MS/MS ion tolerance to 0.3 Da. MS/MS peptide spectra with a minimum ion score confidence interval $>95\%$ were accepted; this was equivalent to a median ion score cutoff of approximately 35 in the data set. Protein identifications were accepted with a statistically significant MASCOT protein search score $>62$ that corresponded to an error probability of $P<0.05$ in our data set.

**Antibodies.** Antibodies used in western blotting: anti-caspase-3, anti-caspase-2, clone 35 and anti-caspase-7, clone B94-1 (all from BD Biosciences, San Jose, CA, USA); anti-cleaved caspase-3 mAb, clone ASP175, anti-profilin and anti-Bid (all from Cell Signaling, Danvers, MA, USA); anti-G3PDH (Nordic Biosite, Stockholm, Sweden); anti-stathmin, anti-tropomyosin anti-myotrophin (all from Santa Cruz Biotechnology, Santa Cruz, CA, USA); anti-ubiquitin (Dako, Stockholm, Sweden). All primary antibodies were diluted in 1 $\times$ PBS containing 1% BSA and 0.05% $NaN_3$. Secondary antibodies were diluted in 2.5% blocking buffer. Horseradish peroxidase-conjugated secondary antibodies were from Thermo Fisher Scientific (Stockholm, Sweden).

**Caspase activity assay.** This assay was performed as described previously.[8] Briefly, $5\times10^5$ cells were washed with 1 $\times$ PBS, resuspended in 25 $\mu$l 1 $\times$ PBS. Fifty microliters of fluorogenic substrates VDVAD-AMC (50 $\mu$M) and DEVD-AMC (50 $\mu$M) were dissolved in reaction buffer (100 mM HEPES (pH 7.25), 10% sucrose, 10 mM DTT, 0.1% CHAPS) and (100 mM MES (pH 6.5), 10% polyethylene glycol, 10 mM DTT, 0.1% CHAPS), respectively. AMC liberation was monitored in a Fluoroscan II plate reader (Labsystems, Vantaa, Finland) using 355 nm excitation and 460 nm emission wavelengths.

**siRNA and plasmids.** Silencing of caspase-2 using siRNA was performed as described before[30] by transfection of 21-nucleotide RNA duplexes. Transfection of anti-caspase-2 (ONTARGETplus SMARTpool L-003465-00-0005; Dharmacon, Lafayette, CO, USA) and control siRNA (sense, 5′-UGAGAAUGUGAUGCGCG UC-TT-3′; Dharmacon) using INTERFERin transfection reagent (Polyplus Transfection, Illkrich, France). Briefly, 10 nmol of double-stranded siRNA (0.55 $\mu$l) and INTERFERin (4 $\mu$l) was mixed in 95 $\mu$l Opti-MEM medium (Invitrogen) and incubated for 10 min at room temperature before added to cells ($2.5\times10^5$). Downregulation of proteins was tested by western blotting. HA-ubiquitin was kindly provided by Dr. A Goldberg (Harvard Medical School, Boston, MA, USA).

**Recombinant protein expression and purification.** pET plasmids containing profilin, stathmin, tropomyosin or myotrophin bearing N-terminal 6 $\times$ His tags were expressed in *Escherichia coli*. Bacteria were inoculated at 37 °C in LB supplemented with antibiotics. When bacterial culture reached an $OD_{600}\sim0.6$, expression were induced by the addition of 1 mM isopropyl $\beta$-D-1-thiogalactopyranoside (Invitrogen) for 6 h at 37 °C. Next, bacteria were pelleted, resuspended in washing buffer (250 mM NaCl, 50 mM $NaH_2PO_4$, 20 mM imidazole, 5 mM $\beta$-mercaptoethanol, 10% glycerol) in the presence of EDTA-free-PIC (Roche Diagnostics GmbH, Stockholm, Sweden) and DNase I (Roche Diagnostics GmbH) and sonicated on ice. Lysates were then cleared by centrifuging at 15 000 $\times$ *g* for 15 min. The supernatant with recombinant proteins was mixed with Ni-NTA agarose beads and incubated at 4 °C overnight and subsequently loaded to an equilibrated column. Bound proteins were eluted by a gradient of imidazole ranging from 20 to 200 mM in washing buffer (250 mM NaCl, 50 mM $NaH_2PO_4$, 200 mM imidazole, 5 mM $\beta$-mercaptoethanol, 10% glycerol).

***In vitro* transcription and translation, TNT-coupled reticulocyte lysate system (Promega, SDS, Falkenberg, Sweden).** [$^{35}$S]Methionine-labeled proteins were synthesized according to the manufacturer's recommendations. Briefly, a mixture of TNT rabbit reticulocyte lysate 25 $\mu$l, TNT reaction buffer 2 $\mu$l, TNT RNA polymerase (T7) 1 $\mu$l, amino-acid mixture (Minus Methionine, 1 mM) 1 $\mu$l, [$^{35}$S]methionine (1000 Ci/mmol at 10 mCi/ml) 2 $\mu$l, RNasin ribonuclease inhibitor (40 U/$\mu$l) 1 $\mu$l, DNA template (0.5 $\mu$g/$\mu$l) 2 $\mu$l and nuclease-free water to a final volume of 50 $\mu$l. The mixture was incubated at 30 °C for 90 min. The radiolabeled proteins were immediately used for *the in vitro* reaction with caspase-2.

## Conflict of Interest

The authors declare no conflict of interest.

**Acknowledgements**. We thank Professor PH Krammer and Dr. I Lavrik for providing us with anti-caspase-8 Abs, Professor MG Grütter and Dr. A Schweizer (University of Zurich, Switzerland) for ankyrin. Dr. J Jung-Ching Lin (The University of Iowa, Iowa City, IA, USA) for pET-tropomyosin plasmid, Dr. D Görlich (ZMBH, Heidelberg, Germany) for pET-profilin and Dr. N Sivasubramanian (The Cleveland Clinic Foundation, Cleveland, OH, USA) for pET-myotrophin plasmid and Jiaqi Huang (Karolinska Institutet) for technical assistance. This work was supported by the Swedish Research Council, the Swedish and the Stockholm Cancer Societies, the Swedish Childhood Cancer Foundation, Swedish Society for Medical Research, the EC FP7 (APO-SYS) programs.

1. Kumar S. Caspase function in programmed cell death. *Cell Death Differ* 2007; **14**: 32–43.
2. Lamkanfi M, Festjens N, Declercq W, Vanden Berghe T, Vandenabeele P. Caspases in cell survival, proliferation and differentiation. *Cell Death Differ* 2007; **14**: 44–55.
3. Kumar S, Kinoshita M, Noda M, Copeland NG, Jenkins NA. Induction of apoptosis by the mouse Nedd2 gene, which encodes a protein similar to the product of the *Caenorhabditis elegans* cell death gene ced-3 and the mammalian IL-1 beta-converting enzyme. *Genes Dev* 1994; **8**: 1613–1626.
4. Yuan J, Shaham S, Ledoux S, Ellis HM, Horvitz HR. The *C. elegans* cell death gene ced-3 encodes a protein similar to mammalian interleukin-1 beta-converting enzyme. *Cell* 1993; **75**: 641–652.

5. Zhivotovsky B, Orrenius S. Caspase-2 function in response to DNA damage. *Biochem Biophys Res Commun* 2005; **331**: 859–867.
6. Ho LH, Read SH, Dorstyn L, Lambrusco L, Kumar S. Caspase-2 is required for cell death induced by cytoskeletal disruption. *Oncogene* 2008; **27**: 3393–3404.
7. Nutt LK, Margolis SS, Jensen M, Herman CE, Dunphy WG, Rathmell JC *et al.* Metabolic regulation of oocyte cell death through the CaMKII-mediated phosphorylation of caspase-2. *Cell* 2005; **123**: 89–103.
8. Vakifahmetoglu H, Olsson M, Orrenius S, Zhivotovsky B. Functional connection between p53 and caspase-2 is essential for apoptosis induced by DNA damage. *Oncogene* 2006; **25**: 5683–5692.
9. Vakifahmetoglu-Norberg H, Zhivotovsky B. The unpredictable caspase-2: what can it do? *Trends Cell Biol* 2010; **20**: 150–159.
10. Kumar S. Caspase 2 in apoptosis, the DNA damage response and tumour suppression: enigma no more? *Nat Rev Cancer* 2009; **9**: 897–903.
11. Baliga BC, Colussi PA, Read SH, Dias MM, Jans DA, Kumar S. Role of prodomain in importin-mediated nuclear localization and activation of caspase-2. *J Biol Chem* 2003; **278**: 4899–4905.
12. Butt AJ, Harvey NL, Parasivam G, Kumar S. Dimerization and autoprocessing of the Nedd2 (caspase-2) precursor requires both the prodomain and the carboxyl-terminal regions. *J Biol Chem* 1998; **273**: 6763–6768.
13. Thornberry NA, Rano TA, Peterson EP, Rasper DM, Timkey T, Garcia-Calvo M *et al.* A combinatorial approach defines specificities of members of the caspase family and granzyme B. Functional relationships established for key mediators of apoptosis. *J Biol Chem* 1997; **272**: 17907–17911.
14. Talanian RV, Quinlan C, Trautz S, Hackett MC, Mankovich JA, Banach D *et al.* Substrate specificities of caspase family proteases. *J Biol Chem* 1997; **272**: 9677–9682.
15. Mancini M, Machamer CE, Roy S, Nicholson DW, Thornberry NA, Casciola-Rosen LA *et al.* Caspase-2 is localized at the Golgi complex and cleaves golgin-160 during apoptosis. *J Cell Biol* 2000; **149**: 603–612.
16. Rotter B, Kroviarski Y, Nicolas G, Dhermy D, Lecomte MC. AlphaII-spectrin is an *in vitro* target for caspase-2, and its cleavage is regulated by calmodulin binding. *Biochem J* 2004; **378**(Pt 1): 161–168.
17. Panaretakis T, Laane E, Pokrovskaja K, Bjorklund AC, Moustakas A, Zhivotovsky B *et al.* Doxorubicin requires the sequential activation of caspase-2, protein kinase Cdelta, and c-Jun NH2-terminal kinase to induce apoptosis. *Mol Biol Cell* 2005; **16**: 3821–3831.
18. Luo X, Budihardjo I, Zou H, Slaughter C, Wang X. Bid, a Bcl2 interacting protein, mediates cytochrome c release from mitochondria in response to activation of cell surface death receptors. *Cell* 1998; **94**: 481–490.
19. Guo Y, Srinivasula SM, Druilhe A, Fernandes-Alnemri T, Alnemri ES. Caspase-2 induces apoptosis by releasing proapoptotic proteins from mitochondria. *J Biol Chem* 2002; **277**: 13430–13437.
20. Sakahira H, Enari M, Nagata S. Cleavage of CAD inhibitor in CAD activation and DNA degradation during apoptosis. *Nature* 1998; **391**: 96–99.
21. Dahal GR, Karki P, Thapa A, Shahnawaz M, Shin SY, Lee JS *et al.* Caspase-2 cleaves DNA fragmentation factor (DFF45)/inhibitor of caspase-activated DNase (ICAD). *Arch Biochem Biophys* 2007; **468**: 134–139.
22. Hermel E, Gafni J, Propp SS, Leavitt BR, Wellington CL, Young JE *et al.* Specific caspase interactions and amplification are involved in selective neuronal vulnerability in Huntington's disease. *Cell Death Differ* 2004; **11**: 424–438.
23. Gu Y, Sarnecki C, Aldape RA, Livingston DJ, Su MS. Cleavage of poly(ADP-ribose) polymerase by interleukin-1 beta converting enzyme and its homologs TX and Nedd-2. *J Biol Chem* 1995; **270**: 18715–18718.
24. Paroni G, Mizzau M, Henderson C, Del Sal G, Schneider C, Brancolini C. Caspase-dependent regulation of histone deacetylase 4 nuclear-cytoplasmic shuttling promotes apoptosis. *Mol Biol Cell* 2004; **15**: 2804–2818.
25. Aho S. Plakin proteins are coordinately cleaved during apoptosis but preferentially through the action of different caspases. *Exp Dermatol* 2004; **13**: 700–707.
26. Oliver TG, Meylan E, Chang GP, Xue W, Burke JR, Humpton TJ *et al.* Caspase-2-mediated cleavage of Mdm2 creates a p53-induced positive feedback loop. *Mol Cell* 2011; **43**: 57–71.
27. Schweizer A, Roschitzki-Voser H, Amstutz P, Briand C, Gulotti-Georgieva M, Prenosil E *et al.* Inhibition of caspase-2 by a designed ankyrin repeat protein: specificity, structure, and inhibition mechanism. *Structure* 2007; **15**: 625–636.
28. Karki P, Dahal GR, Shin SY, Lee JS, Cho B, Park IS. Efficient cleavage of Bid and procaspase-7 by caspase-2 at lower pH. *Protein Pept Lett* 2008; **15**: 1044–1049.
29. Wejda M, Impens F, Takahashi N, Van Damme P, Gevaert K, Vandenabeele P. Degradomics reveals that cleavage specificity profiles of caspase-2 and effector caspases are alike. *J Biol Chem* 2012; **287**: 33983–33995.
30. Olsson M, Vakifahmetoglu H, Abruzzo PM, Hogstrand K, Grandien A, Zhivotovsky B. DISC-mediated activation of caspase-2 in DNA damage-induced apoptosis. *Oncogene* 2009; **28**: 1949–1959.
31. Mhaidat NM, Thorne RF, de Bock CE, Zhang XD, Hersey P. Melanoma cell sensitivity to docetaxel-induced apoptosis is determined by class III beta-tubulin levels. *FEBS Lett* 2008; **582**: 267–272.
32. Ark M, Ozdemir A, Polat B. Ouabain-induced apoptosis and Rho kinase: a novel caspase-2 cleavage site and fragment of Rock-2. *Apoptosis* 2010; **15**: 1494–1506.
33. Kong JY, Rabkin SW. Cytoskeletal actin degradation induced by lovastatin in cardiomyocytes is mediated through caspase-2. *Cell Biol Int* 2004; **28**: 781–790.
34. Ndozangue-Touriguine O, Hamelin J, Breard J. Cytoskeleton and apoptosis. *Biochem Pharmacol* 2008; **76**: 11–18.
35. Burnett BG, Andrews J, Ranganathan S, Fischbeck KH, Di Prospero NA. Expression of expanded polyglutamine targets profilin for degradation and alters actin dynamics. *Neurobiol Dis* 2008; **30**: 365–374.
36. Liu Z, Lu H, Shi H, Du Y, Yu J, Gu S *et al.* PUMA overexpression induces reactive oxygen species generation and proteasome-mediated stathmin degradation in colorectal cancer cells. *Cancer Res* 2005; **65**: 1647–1654.
37. Norberg E, Karlsson M, Korenovska O, Szydlowski S, Silberberg G, Uhlen P *et al.* Critical role for hyperpolarization-activated cyclic nucleotide-gated channel 2 in the AIF-mediated apoptosis. *EMBO J* 2010; **29**: 3869–3878.
38. Perdomo AB, Ciccosanti F, Iacono OL, Angeletti C, Corazzari M, Daniele N *et al.* Liver protein profiling in chronic hepatitis C: identification of potential predictive markers for interferon therapy outcome. *J Proteome Res* 2012; **11**: 717–727.